LAWRENCE
LIVERMORE
NATIONAL
LABORATORY

UCRL-JRNL-236544

Predictive three dimensional modeling of Stimulated Brillouin Scattering in ignition-scale experiments

L. Divol, R. Berger, N. Meezan, D. H. Froula, S. Dixit, L. Suter, S. H. Glenzer

November 14, 2007

Physics Review Letters

Disclaimer

Predictive three dimensional modeling of Stimulated Brillouin Scattering in ignition-scale experiments

L. Divol, R. L. Berger, N. B. Meezan, D. H. Froula, S. Dixit, L. Suter and S. H. Glenzer
L-399, Lawrence Livermore National Laboratory,
University of California P. O. Box 808, CA 94551, U.S.A.
(Dated: November 7, 2007)

The first three-dimensional (3D) simulations of a high power 0.351μm laser beam propagating through a high temperature hohlraum plasma are reported. We show that 3D linear kinetic modeling of Stimulated Brillouin scattering reproduces quantitatively the experimental measurements, provided it is coupled to detailed hydrodynamics simulation and a realistic description of the laser beam from its millimeter-size envelop down to the micron scale speckles. These simulations accurately predict the strong reduction of SBS measured when polarization smoothing is used.

PACS numbers: PACS numbers: 52.40.Nk, 52.35.Mw, 05.10.Gg, 02.50.Ey

One of the grand challenge of laser-plasma interaction (LPI) studies is to provide guidance for the design of hohlraum targets on the next generation of laser facilities for ignition attempts [1, 2, 4]. Modeling LPI processes in real-size experiments has been recognized as a difficult task. One of the main difficulties is the vast parameter space in electron density, temperature and spatial scales that are typically spanned by an ignition relevant laser-plasma experiment on current laser facilities. This leads to a plethora of (usually coupled) LPI processes such as absorption, refraction, diffraction, filamentation and parametric backscattering instabilities[3]. Another challenge is the proper description of the spatially smoothed laser beams used on all modern facilities, which exhibit intensity structures from the hundreds of microns down to the micron scale[5].

There are two main numerical modeling approaches for LPI. Particle-in-cell or Focker-Plank type codes solve consistently a set of Maxwell-Vlasov-like equations and are limited to short timescales (picoseconds), small plasma volumes (typically one laser speckle) or low dimensionality (1 or 2 dimensions). While 3-dimensional PIC simulations of diffraction limited short pulse experiments are becoming common tasks due to increasingly powerful computers, long pulse (nanosecond) ignition scale (cubic millimeter) LPI experiments are still out of reach for such numerical tools. Another approach is to use a fluid-based description of LPI processes[6–8, 11]. This allows relaxing both spatial and temporal resolutions and no discretization in particle velocity space is required.

In this letter, we report on the first three dimensional simulations of a whole laser beam propagating through an ignition-scale experiment, using the fluid paraxial code pF3d. These simulations include models for both stimulated Raman (SRS) and Brillouin (SBS) backscattering. We show that a fluid-based modeling of SBS including linear kinetic correction, coupled to accurate hydrodynamics profiles and a realistic description of the laser intensity pattern generated by various smoothing options leads to quantitative agreement between the measured and calculated reflectivities over many order of magnitude and for different smoothing techniques (polarization smoothing and smoothing by spectral dispersion).

We are interested here in validating LPI modeling tools in conditions close to future ignition experiments. In this letter we model a series of recent experiments[12] performed at the Omega laser facility (LLE/Rochester). An interaction beam propagating along the axis of a hydrocarbon-filled hohlraum heated by up to 17 kJ of heater beam energy interacts with a millimeter-scale underdense ($N_e = 6.5\%$ critical) uniform plasma at electron temperatures T_e around 3 keV. The interaction beam power was varied between 50 and 500 GW, at a wavelength of $\lambda_0 = 0.351\mu m$. Using a 150 μm CPP, the average intensity on axis was varied between 5 $10^{14} W.cm^{-2}$ and 4 $10^{15} W.cm^{-2}$. Absolutely calibrated diagnostics measure the backscattered light. These laser-plasma conditions are close to those encountered in current ignition hohlraum designs.

A number of steps are necessary in order to confidently compare pF3d simulation results with the measured reflectivities.

First we need accurate plasma parameters as input for pF3d. Extensive Thomson scattering measurements [13] in the multispecies plasma (C and H atoms) allowed to measure both the electron and ion temperatures at the center of the target, as well as the density evolution. These time-resolved measurements were successfully compared to HYDRA simulations and show relative insensitivity to the exact heat conduction model employed[14]. We can then directly use HYDRA three-dimensional hydrodynamics maps (electron density Ne and temperature Te, ion temperature Ti and plasma flow) as initial conditions for pF3d. We perform post-shot HYDRA simulations to account for variation in heater beam energy (typically $< 4\%$) and gas fill pressure ($< 10\%$) between shots. Figure 1 shows the plasma parameters along the hohlraum axis as used in the simulation. The transverse variations were also included.

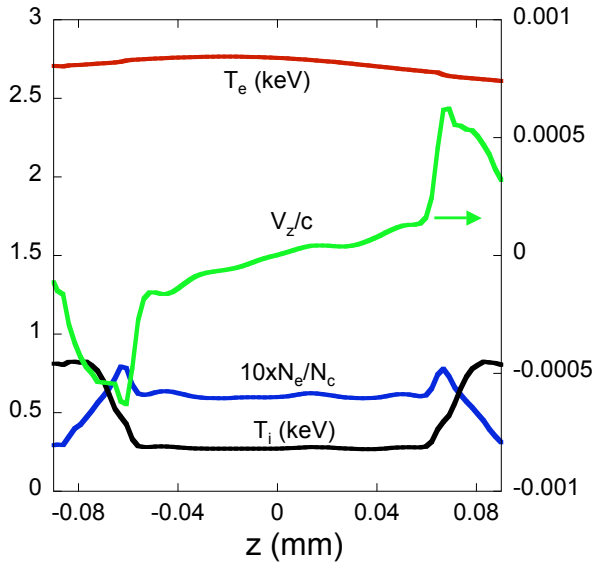

FIG. 1: Plasma parameters at t=700 ps along the hohlraum axis calculated by HYDRA. Electron density, temperature, ion temperature and flow are used as initial conditions for pF3d simulations.

We chose to model the experiment at a time when the plasma electron temperature is close to 3 keV and the density profile is relatively uniform.

Second, a realistic description of the laser beam is needed. We use the measured continuous phase plate (CPP) phase mask used on the interaction beam and a model for Omega beam aberrations. Figure 2 shows transverse and longitudinal slices through the middle of the resulting beam intensity while Fig. 2c shows a 3D rendering of the laser beam propagating through the plasma. The simulation resolves both the envelop of the beam, which is close to a Gaussian with 150 μm FWHM at best focus and the f/6.7 speckles at the micron scale. The typical resolution required by the paraxial approximation used for laser propagation is $dx = dy = 1.3\lambda_0$ and $dz = 4\lambda_0$. The plasma volume modeled encompasses more than a billion cells. It is difficult to define an average laser intensity for such a beam, but a benefit of 3D whole beam simulations is that only the beam power (here in the 100-400 GW range) is needed as an input parameter. As a reference, the intensity averaged over a 50 μm^3 volume at best focus is 1.15 $10^{15} W.cm^{-2}$ for an input power of 100 GW. Additional beam smoothing techniques are equally accurately modeled. When polarization smoothing (PS)[15] is used, pF3d solves paraxial equations for each polarization component, with the two speckle patterns being offset in the far field by the experimentally measured shift induced by the PS wedge. Smoothing by spectral dispersion (SSD)[16] is modeled using the correct modulator, grating geometry and depth of modulation.

Third, a detailed fluid-based model has been developed to describe the response of the plasma to the ponderomotive drive and is described in [berger98]. Here we will focus on the details of the SBS model which was dominant in the experiment. Stimulated Raman backscatter was below measurement threshold for all powers and negligible in simulations too, as expected in low density, high temperature plasmas where Landau damping is large. The electron density perturbation δn associated with the SBS-driven acoustic wave is enveloped in space at $k_a = 2k_0$, but not in time to describe correctly the modified decay regime when the SBS growth rate becomes larger than the acoustic frequency ω_a in high intensity speckles. The resulting differential equation is :

$$(\partial_t + u.\nabla + 2ik_0u_z + \nu_a)^2\delta n$$
$$+(\omega_a^2 - 2ik_0c_a^2\partial_z - c_a^2\nabla^2)\delta n = \gamma_a a_0 a_1^* \qquad (1)$$

where a_0 (resp. a_1) are the normalized field amplitude of the incoming (resp. backscattered) light. The Vlasov-Landau kinetic dispersion relation for SBS-driven ion-acoustic waves at $k = k_a$ is solved at each position in the plasma to account for detuning due to all plasma parameters and the most unstable local solution provides the local acoustic frequency ω_a and Landau damping ν_a. The sound speed is defined as $c_a = \omega_a/k_a$. At the center of the target, the values are $\omega_a = 13ps^{-1}$ and $\nu_a = 0.15\omega_a$.The coupling coefficient γ_a is obtained by matching the resulting convective amplification to the 1D fully kinetic result. This linear kinetic treatment of SBS-driven acoustic waves provides a correct description of the time evolution of SBS, which is important to correctly model the coupling to other time-dependent LPI processes such as filamentation and SRS and the effect of temporal beam smoothing. Ion-acoustic waves in a multi-ion-species plasma are described by an aver-

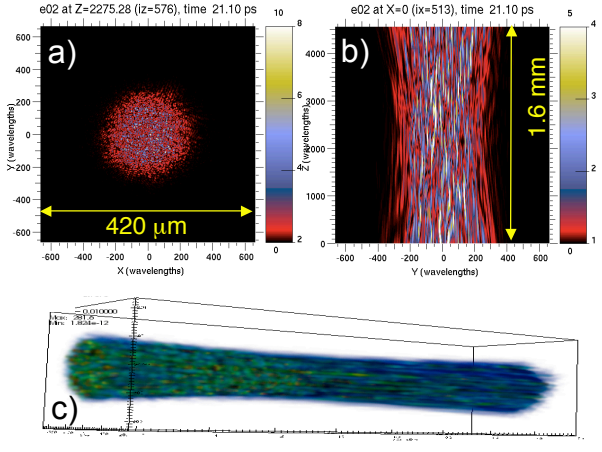

FIG. 2: Beam intensity profiles in a plane perpendicular to the direction of propagation (a, at best focus) and parallel (b). three dimensional rendering of the whole beam as simulated by pF3d (c)

age (most-unstable) mode. This model also recovers the exact steady-state gain exponent, which is necessary for quantitative comparisons with experiments. It is accurate as long as the ion-acoustic wave amplitude is small enough to neglect kinetic (trapping) and fluid(harmonics, decay,...) nonlinearities and the electron temperature is high enough to neglect collisional corrections to our kinetic approach (such as non-local heat transport). The later condition is fulfilled in the low density, mid-Z, high temperature experiment (see Fig. 2) described in this letter, as it is in ignition-hohlraum mid-Z plasmas for all current ignition designs.

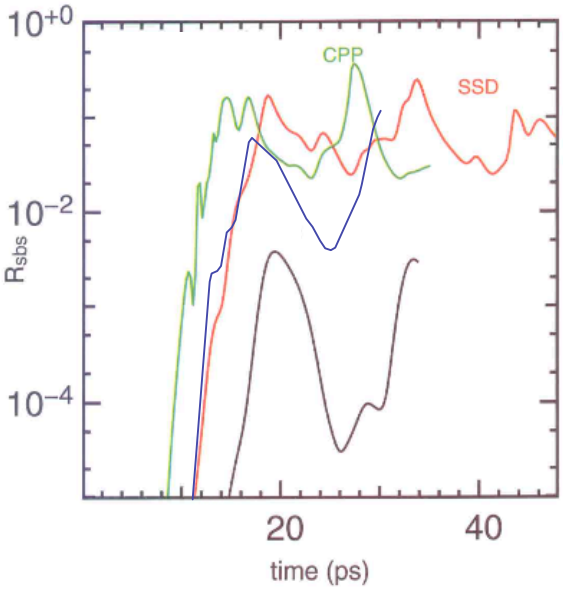

FIG. 3: pF3d calculated SBS reflectivity as function of simulation time for a laser power of 175 GW. (green) is with CPP only, (red) with 3 A of SSD bandwidth and (black) with PS. (blue) corresponds to CPP-only at 130 GW.

Our approach to simulating SBS consists in using 3D hydrodynamics parameters from an integrated HYDRA simulation of the entire hohlraum as initial conditions for pF3d. This is justified by the separation of time scales between the evolution of the gross hydrodynamics simulated by HYDRA (100 ps) and the LPI processes simulated by pF3d (10 ps). The pF3d simulation is then run for a few tens of picosecond on a plasma volume encompassing the interaction beam, until SBS reaches a statistical steady state. Fig 3. shows that while fast oscillations remains in the reflectivity, a well defined average emerges after 20 picoseconds for various intensities. We define the pF3d reflectivity as the average between 20 ps and 50 ps. The fact that we can start the pF3d simulation at 700 ps without prior knowledge of the SBS evolution is justified by an experiment where the interaction beam was delayed by 200 ps and the measured SBS was shown to coincide with the non-delayed measurement[14]: SBS in this CH plasma is in the strongly damped regime and reacts almost instantly (over 10 ps) to local laser-plasma conditions.

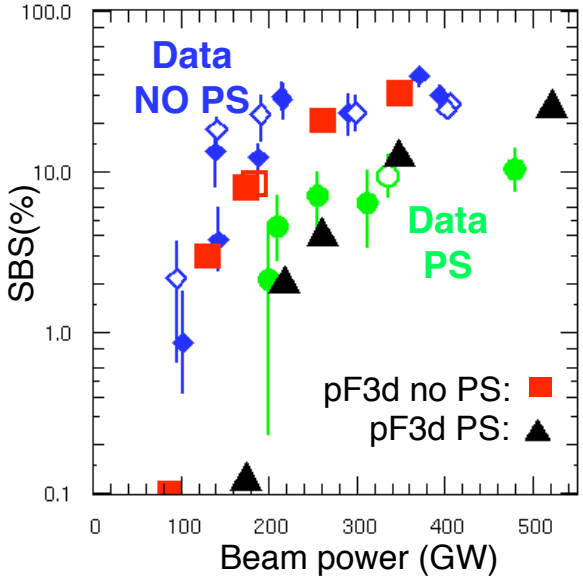

FIG. 4: Measured (blue diamonds and green circles) and calculated (red squares and black triangles) SBS reflectivity as function of laser power at t=700 ps. Both the measurement and simulations show a factor of two increase in the SBS threshold when PS is used. Empty symbols corresponds to measurements and simulations with 3Å of SSD added. pF3d results quantitatively match the measured reflectivity over more than two order of magnitude for all smoothing techniques employed.

Figure 4 shows the measured and simulated SBS reflectivity as function of the interaction beam power. It is worth noting that our modeling doesn't allow for any free parameter: the laser and plasma parameters used as boundary and initial conditions are given by measurements or integrated simulations validated by measurements, while the SBS model is closed and derived from first principle linearized equations. The calculated Pf3D SBS reflectivities agree quantitatively with measurements over more than 2 order of magnitudes. pF3D predicts correctly the large increase in the SBS threshold when PS is used, as well as the absence of any measurable reduction of SBS when 3Å of SSD is added. The SBS signal simulated is almost entirely contained in the beam f-cone, which is consistent with the experiment. As Fig. 3 shows, the reflectivity oscillates regularly with a period of approximately 12 ps. The source of these oscillations can be traced back to a few very intense speckles in the back of the plasma. The light scattered by these speckles, while representing a modest amount of power, acts as a seed for SBS that is amplified through the plasma. The resulting pump depletion happening at the front of the plasma due to this enhanced SBS makes these speckles in

the back of the plasma blink, which leads to oscillations with a period close to four times the transit time of light through the plasma. We turned off the filamentation instability in a few simulations and while the reflectivity was reduced near threshold, the overall result was very close to Fig.4. This is consistent with the high electron temperature and moderate laser intensity, which results in weak self-focusing of speckles and limited change to the beam contrast.

Thus, the factor of 2 increase in the SBS threshold when PS is used is not due to a control of the filamentation instability[17] but to a direct mitigation of the SBS growth. Indeed, the average laser intensity doesn't exceed the so-called critical intensity for SBS (corresponding to an e-fold amplification over one speckle length) until very large reflectivity are observed. In this regime of low amplification over any speckle, a single row of speckles can act as an enhanced noise source but has a negligible contribution in the overall reflectivity, which is determined by amplification over many successive rows. When PS is used, on average only one or the other polarization is amplified over any speckle, which leads in the limit of small amplification per speckle to a reduction of 2 of the overall gain exponent throughout the whole plasma. This is observed both in the experiment and in the simulations (Fig. 4).

Using 3 Å of SSD bandwidth has no significant effect on SBS, both in the experiment and in simulations. This can be expected in this strongly damped regime where the damping rate ν_a is almost 10 times larger than the inverse correlation time introduced by the laser bandwidth. The situation could be quite different in a weakly damped regime, such as in the gold plasma close to the hohlraum wall[18]. Previous observations of SBS reduction through control of filamentation by SSD does not apply to this high T_e, moderate intensity experiment, as noted before.

The validity of our description of SBS-driven ion-acoustic waves relies on their amplitude remaining small. To quantify this, we have computed the distribution of the wave amplitude $\delta n/n_e$ in a transverse plane close to the entrance of the plasma, where the average amplitude peaks (as the instability grows from the back of the plasma). For a laser power of 150 GW and smoothing with CPP only, a reflectivity of about 8% was calculated and we find that 1% (resp. 10%) of the transverse plane is occupied by waves with amplitudes above 1% (resp. 0.3%). The maximum amplitude observed is 3%. Fluid nonlinearities scale usually with $(\delta n/n_e)^2$ and are thus negligible[19, 20]. These amplitudes are also well below the two-ion decay instability threshold $\delta n/n_e > 4\nu_a \approx 60\%$[21] and the wave-breaking limit. Trapping of electron or hydrogen ions in the SBS-driven ion-acoustic wave could lead to a change in Landau damping and a frequency shift[**?**]. The frequency shift induced by electron trapping scales as $\delta\omega/\omega_a \approx 0.2(\delta n/n_e)^{-0.5}$ and a similar result is expected for trapping of hydrogen ions. This is a 1% effect for $\delta n/n_e = 0.3\%$ and is much smaller than the linear damping rate ν_a, thus negligible. The last effect could be a reduction of Landau damping in intense speckles. By comparing the bouncing period of protons in an acoustic wave with the transit time of a proton crossing a speckle and with the detrapping timescale due to H-C collisions, one finds that trapping of protons could occur for $\delta n/n_e$ as low as 0.3% with the parameters of Fig. 1. Thus up to 10% of the plasma at the front of the target could be subject to trapping effect (this is still less than 1% of the overall simulation volume). One could then question the validity of our SBS model above 150 GW for CPP-only (and above 300 GW for CPP+PS), but as reflectivities are already large and the physics is dominated by whole-beam pump depletion, the experimental measurement is not discriminative. Nonlinear saturation effects missing in our model could also explain the discrepancy observed at very high power (Fig. 4 around 500 GW). We are not claiming that our modeling tools are accurate at such high intensity and large reflectivities.

While developing a general predictive modeling capability for LPI remains a challenge, we have made a significant step towards that goal by using a detailed description of the plasma conditions and the laser beam intensity pattern as input to full 3D fluid-based LPI simulations done with our massively parallel code pF3d. This experimental validation is for now limited to stimulated Brillouin backscatter in a regime where kinetic and fluid nonlinearities are not expected to play a significant role (long hot plasma at moderate density and laser intensity). This is a regime of interest for forthcoming attempts at ignition on NIF and LMJ.

This work was performed under the auspices of the U.S. Department of Energy by Lawrence Livermore National Laboratory in part under Contract W-7405-Eng-48 and in part under Contract DE-AC52-07NA27344.

[1] Moses, E. I. and Wuest C. R. Fusion Sci. Tech. 47, 314-322 (2005).
[2] Cavailler, C. Fusion 47, B389-B403 (2005).
[3] Kruer,W. L. The Physics of Laser Plasma Interaction (Addison-Wesley, New York, 1988)
[4] Lindl, J. D. *et al.*, Phys. Plasmas 11, 339 -491 (2004).
[5] Still, C. H. *et al.*, Phys. Plasmas 7, 2023-2032 (2000).
[6] Huller, S. Mounaix, Ph. and Pesme, D. Phys. Scr. T63, 151-157 (1996).
[7] Schmitt, A. J. and Afeyan B. B. Phys. Plasmas 5, 503-517 (1997).
[8] Myatt, J. *et al.*, Phys. Plasmas 11, 3394-3403 (2004).
[9] Loiseau, P. Phys. Rev. Lett. 97, 205001 (2006)
[10] Pesme, D. *et al.*, Plasma Phys. Controlled Fusion 44, B53 (2002)
[11] Berger, R. L. *et al.*, Phys. Plasmas **5**, 4337 (1998)
[12] Froula, D. H. *et al.*, Phys. Rev. Lett. 98, 085001 (2007).

[13] Froula, D. H. *et al.*, Phys. Plasmas **14**, 055705 (2007)
[14] Meezan, N. B. *et al.*, Phys. Plasmas **14**, 056304 (2007)
[15] Tsubakimoto, K. *et al.*, Opt. Commun. 91, 9-12 (1992).
[16] Skupsky, S. *et al.*, J. Appl. Phys. 66, 3456-3462 (1989).
[17] Lefebvre, E. *et al.*, Phys. Plasmas 5, 2701- 2705 (1998)
[18] Divol, L. Phys. Rev. Lett. 99, 155003 (2007).
[19] Heikkinen, J. A. *et al.*, Phys. Fluids 27, 707-720 (1984).
[20] Rozmus, W. *et al.*, Phys. Fluids B 4, 576-593 (1992).
[21] Niemann, C. *et al.*, Phys. Rev. Lett. 93, 045004 (2004)
[22] Riconda, C. *et al.*,Phys. Rev. Lett. 94, 055003 (2005).